9th International Conference on NDT of Art, Jerusalem Israel, 25-30 May 2008
For more papers of this publication click: www.ndt.net/search/docs.php3?MainSource=65

MICRO-ANALYTICAL STUDY OF THE MORDANT GILDING TECHNIQUE IN THREE POST-BYZANTINE CHURCHES IN THESSALIA, GREECE

Olga Katsibiri [1], Russell F. Howe [2]
[1] Department of Conservation, National Gallery of Athens
Michalakopoulou 1, 115 28 Athens, Greece
Tel: +30 210 7235937-8, Fax: +30 210 7224889, E-mail: o.katsibiri@gmail.com
[2] Department of Chemistry, University of Aberdeen
Meston Walk, Old Aberdeen, Aberdeen AB24 3UE, Scotland, U.K.

ABSTRACT
The wall paintings from the main churches of three monasteries in Thessalia, Central Greece, all painted in the post-Byzantine period, were investigated using micro-analytical techniques. The main goal was to offer insights into the decorative technique of mordant gilding and to provide evidence on the identity of the painter.

INTRODUCTION
In the preparation of wall paintings, specific features of the representations were often decorated with gold. For this application, the gold leaf was usually attached onto the areas to be gilded by means of a mordant [1]. This technique, however, has scarcely been investigated and as yet very little is known about its application in Byzantine wall painting.

The wall paintings investigated in this study derive from the main churches of three monasteries in Thessalia, Central Greece and were all painted in the post-Byzantine era, more specifically between 1552 and 1560. In particular, the main church of the St. Byssarionas Monastery at Doussiko was painted in 1557 by Tzortzis, one of the most important iconographers associated with the Cretan School [2-4]. The main church of the Transfiguration Monastery (Great Meteoro) belongs to the monastic community of Meteora. Its mural decoration was completed in 1552, with the exception of the older-constructed sanctuary, and it is considered to be a masterpiece of the Cretan School [5-7]. Lastly, the Roussanos Monastery is also part of Meteora. Its main church was decorated in 1560 with wall paintings that represent the mature artistic production of the Cretan School [8,9].

Samples were taken from the gilded decoration of several saints depicted in the three churches. The stratigraphy was first viewed in cross-sections using light microscopy (LM). The chemical composition was then determined by electron ionisation direct temperature resolved mass spectrometry (EI-DTMS). This technique led to the detection of the organic compounds and some of their degradation products formed during ageing, as well as of certain inorganic materials. To increase sensitivity towards oxidised molecules, positive ammonia chemical ionisation (NH_3/CI) conditions were also applied. The metal constituents were detected by scanning electron microscopy – energy dispersive X-Ray spectroscopy (SEM-EDX).

The main objectives of this study are the characterisation of the mordants, in terms of function, properties, and chemical composition, as well as the study of the deterioration changes occurred due to ageing. Furthermore, the layer build-up and the chemical composition of the mordants were compared to check on and possibly provide evidence on the identity of the painter in the three churches.

EXPERIMENTAL

Samples

Forty-five (45) samples of approximate 1mm^2 each were taken from thirteen (13) post-Byzantine wall paintings. The samples were classified into three categories according to the areas they were taken from, namely the haloes, and the linear and bulk decoration of the garments (Fig. 1). Special care was taken that samples were removed from areas that were already damaged. After observing the samples under the stereomicroscope, cross-sections were prepared by mounting them in Technovit ® 2000 LC, a one-component methacrylate that polymerises in blue light. Wet grinding with silicone carbide (SiC) sheets followed and their surface was dry-polished on Micro-Mesh ® cloths [10].

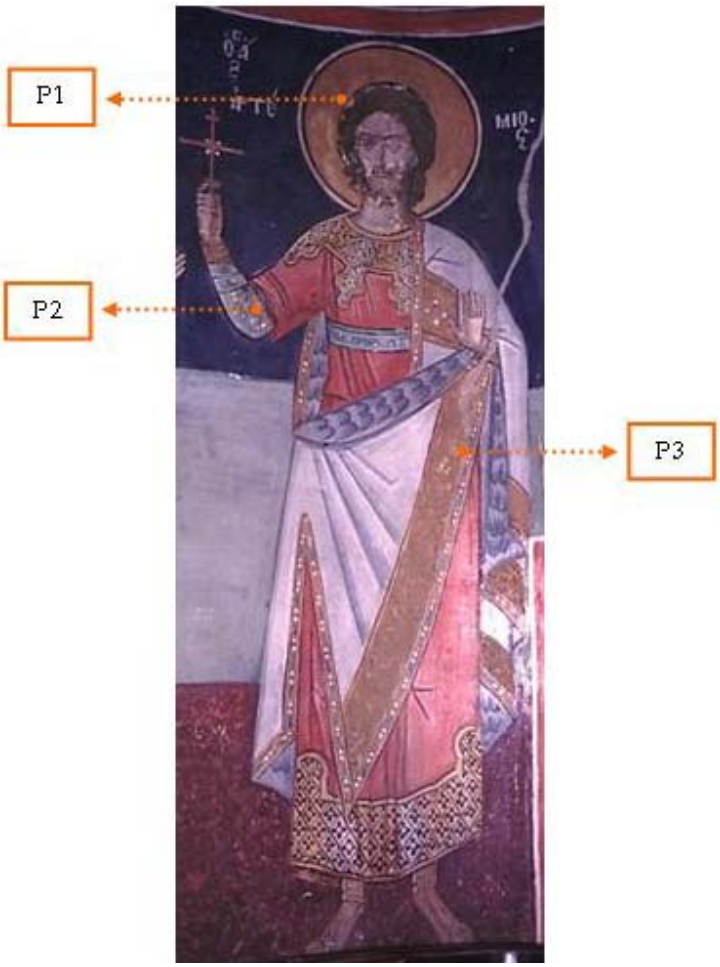

Fig. 1 – The three categories of sample areas from St. Artemios (size: 1.50 x 0.54), main church of the Roussanos monastery

LM

The cross-sections were observed under a Leica DMRX analytical microscope (Leica Inc., Wetzlar, Germany) with a resolution of approximately 1 μm. The microscope was equipped with a 100 W halogen projection lamp for visible (VIS) incident light microscopy in bright and dark field illumination. For ultra-violet (UV) fluorescence microscopy, an Osram HBO 50 high-pressure mercury lamp and a Leica filter D (excitation 360-425 nm, emission > 460 nm) were used. The cross-sections were recorded in images with a Nikon DXM1200 digital still camera (Nikon Instech Co., Ltd., Japan).

EI-DTMS and NH3/CI-DTMS

Sub-sampled layers of about 10-50 μg were made into a suspension in a mini-mortar using aliquots of ethanol. Approximately 2-5 μl of the suspension was transferred to the platinum/rhodium (90:10) filament (∅ 100 μm) of the probe, dried in vacuo, and inserted directly into the ion source of a JEOL JMS-SX/SX102A tandem mass spectrometer. The filament was resistively heated by ramping the current at a rate of 0.5 A/min, and the temperature linearly increased from ambient to approximately 800 ºC in 2 min. Ions were generated using 16 eV EI.

Selected samples were derivatised in a 2.5 % w/v methanolic solution of tetramethylammonium hydroxide (TMAH), added to them for methylation to observe better the diacid distribution. Desorbed and pyrolysed material was ionised under NH_3/CI conditions which, compared to EI conditions, cause less fragmentation and thus provide more information on the molecular ions. The mass spectrometer was scanned over a m/z range of 60-1000 using a 1 s cycle time.

SEM-EDX

The cross-sections were carbon coated on a CC7650 Polaron Range coater with carbon fibre (Quorum Technologies, East Sussex, UK) to improve surface conduction. Measurements were performed on a XL30 SFEG high-vacuum electron microscope equipped with a field emission source (FEI, Eindhoven, The Netherlands) and an EDX system from EDAX (Tilburg, The Netherlands). Information on elemental composition was obtained by spot analysis. Backscatter electron (BSE) images were taken at 20 kV acceleration voltage, 5 mm eucentric working distance, and a spot size of 3, corresponding to a beam diameter of 2.2 nm with current density of approximately 130 pA. EDX analysis was performed at a spot size of 4 (beam diameter 2.5nm, current density 550 pA) and at acceleration voltage of 22 kV to obtain higher count rate.

RESULTS AND DISCUSSION

LM

All samples consist of a golden-brown mordant layer of variable thickness (circa 3-123 μm) that was used to attach the gold leaf (2-7 μm). In the majority of samples from the saints' gilded haloes, there is a light- to golden-yellow layer below the mordant that appears to play the role of the bole to the gold leaf (Fig. 2a,b). In some cases, however, the paint layer corresponding to the background where the saints were painted on is seen directly underneath the mordant (Fig. 2c,d). In most of the samples taken from the gilded linear decoration of the saints' garments, a white layer is seen underneath the mordant that, together with the paint layer below, correspond to the garments (Fig. 3a,b). In many cases, however, the mordant is seen applied directly over the paint layer of the garments (Fig. 3c,d). Finally, in the majority of samples taken from the gilded bulk decoration of the saints' garments, a light- to golden-yellow layer is observed again below the mordant (Fig. 4a,b). In a number of cases, however, several paint layers that correspond to the garments are seen either alone or in-between the mordant and that yellow layer. Amongst those, there is a black-paint layer that appears to be part of a black-pattern decoration underneath the gilding (Fig. 4c,d). It therefore seems that most of these areas had been initially embellished with black motifs on a yellow background, and then covered with gilding at a later stage (Fig. 1).

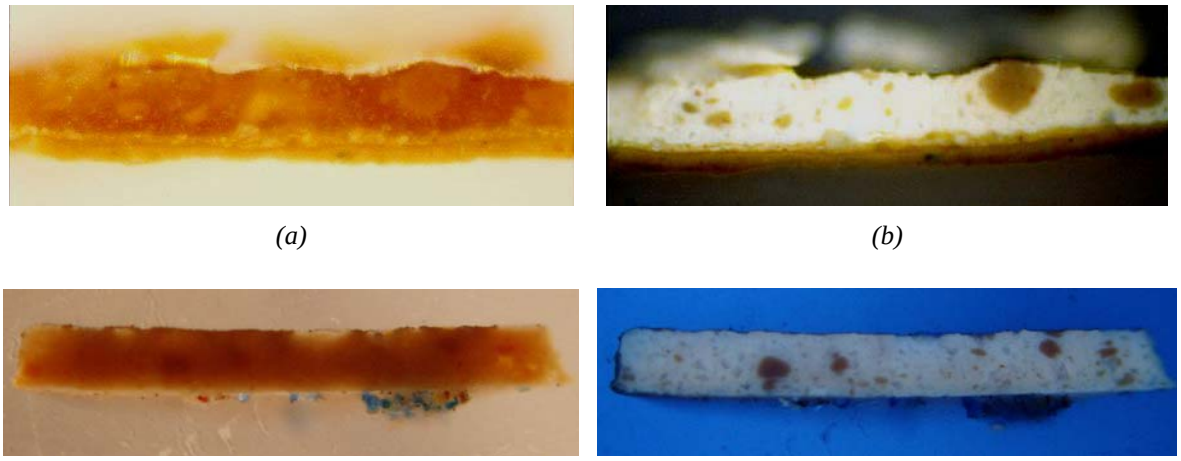

(a) *(b)*

(c) *(d)*

Fig. 2 – Gilded haloes
Top row: cross-section of sample S1, magnification 200x, illumination in (a) VIS incident light (b) UV light
Bottom row: cross-section of sample M10, magnification 10x, illumination in (c) VIS incident light (d) UV light

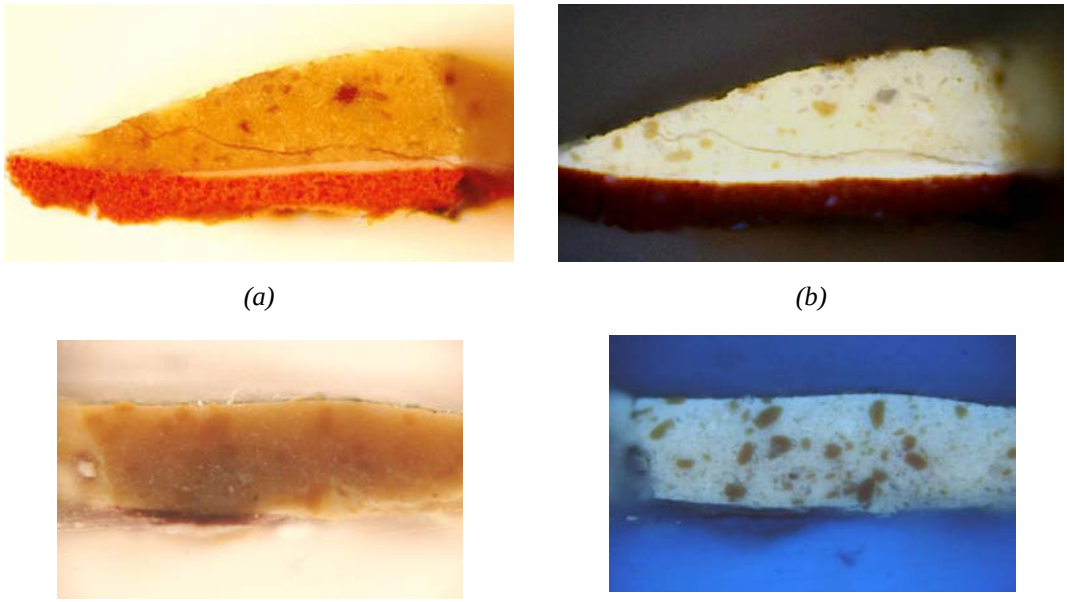

(a) *(b)*

(c) *(d)*

Fig. 3 – Gilded linear decoration of the garments
Top row: cross-section of sample S5, magnification 200x, illumination in (a) VIS incident light (b) UV light
Bottom row: cross-section of sample P8, magnification 10x, illumination in (c) VIS incident light (d) UV light

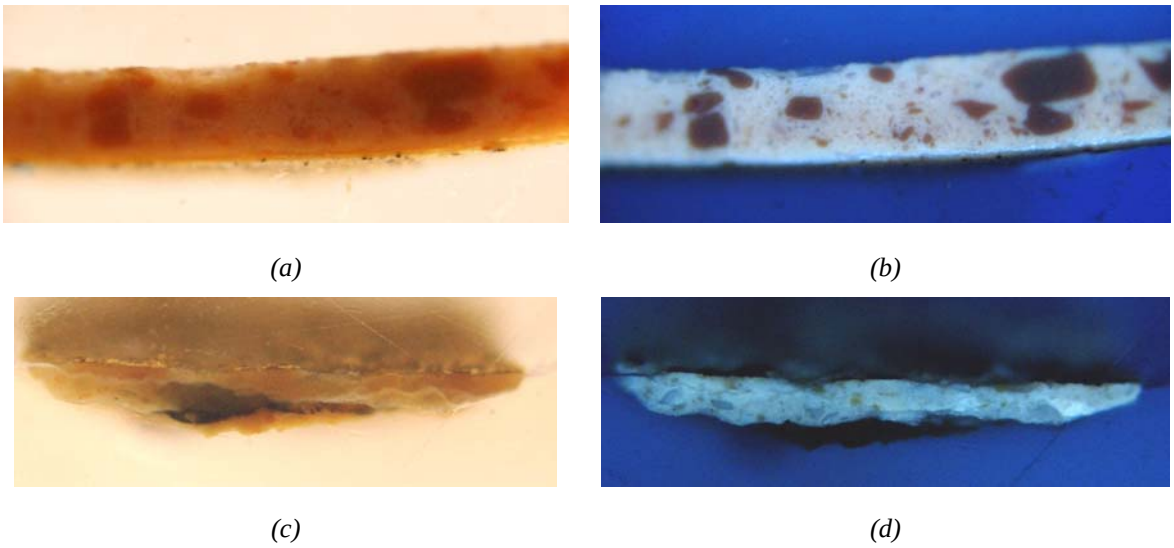

Fig. 4 – Gilded bulk decoration of the garments
Top row: cross-section of sample M3, magnification 10x, illumination in (a) VIS incident light (b) UV light
Bottom row: cross-section of sample P3, magnification 10x, illumination in (c) VIS incident light (d) UV light

EI-DTMS and NH3/CI-DTMS

All the mordants analysed contain a drying oil, as results from the summation mass spectra (Fig. 5a). In particular, observed at *m/z* 256 and *m/z* 284 are the molecular ions of the C16:0 fatty acid (FA) (palmitic acid) and the C18:0 FA (stearic acid), respectively. In the majority of cases, the mass peaks at *m/z* 73, 83, 98, 111, 129, 143, 171, 185, 213, and 241 are also present that derive from fragmentation of FA components. Moreover, at *m/z* 91 and 105 the fragment ions of alkylated benzenes are detected that are generated from a polymeric oil-derived network. These are seen predominantly in the pyrolysis region of the total ion currents (TICs) (Fig. 5b,c) [11].

The ratio of the molecular ions of the palmitic (C16:0) to the stearic (C18:0) acids (P/S) is considered to be a relatively stable feature and can thus be used to identify the type of drying oil. From the values of this ratio and after comparing them with the literature values, it seems that in all cases linseed oil has been used for the preparation of the mordants [12].

Furthermore, the two above-mentioned mass peaks in the low temperature region of the TICs reveal the presence in the majority of mordants of free FAs (Fig. 5c). These must have been released from the oil network due to hydrolysis of the initial triacylglycerol ester bonds [13]. This piece of information is supported by the fact that no characteristic peaks of mono-, di- or triacylglycerols were detected in the summation mass spectra (partially seen in Fig. 5a). On the other hand, the high intensity of the pyrolysis peak in the TICs as opposed to the low intensity of the desorption region indicates that the mordants consist primarily of pyrolysed polymeric material rather than low-molecular-mass desorbing compounds (Fig. 5c).

In addition, azelaic acid (C9 diacid) was detected in all cases by its most characteristic and intense EI fragment ion at *m/z* 152 (Fig. 5c) [14]. This diacid is a relatively stable end product formed upon oxidation of the unsaturated FAs present in fresh oil, and as such it is encountered in aged oil-paint systems. Given that the amount of palmitic acid remains constant, the azelaic to palmitic acids ratio (Az/P) can constitute an indicator of the oxidation state of a dried-oil film. The values of this ratio being below 1, the amount of azelaic acid is relatively low, and it therefore seems that the mordants have not oxidised extensively.

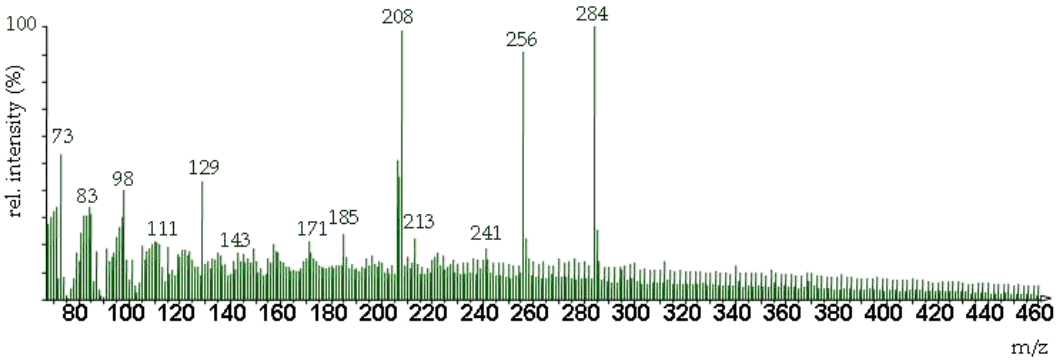

(a)

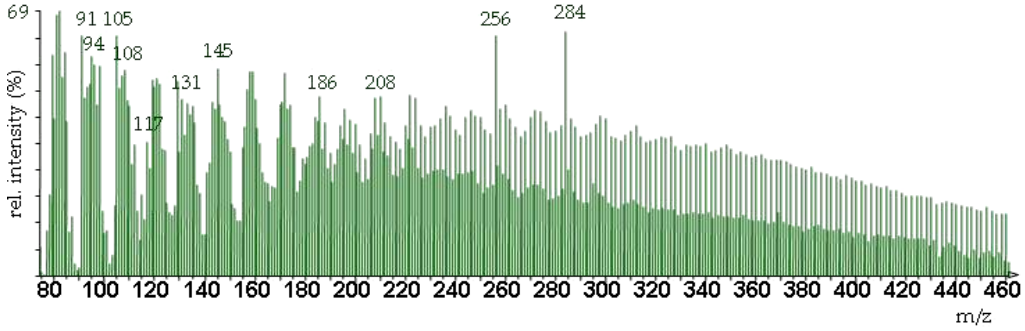

(b)

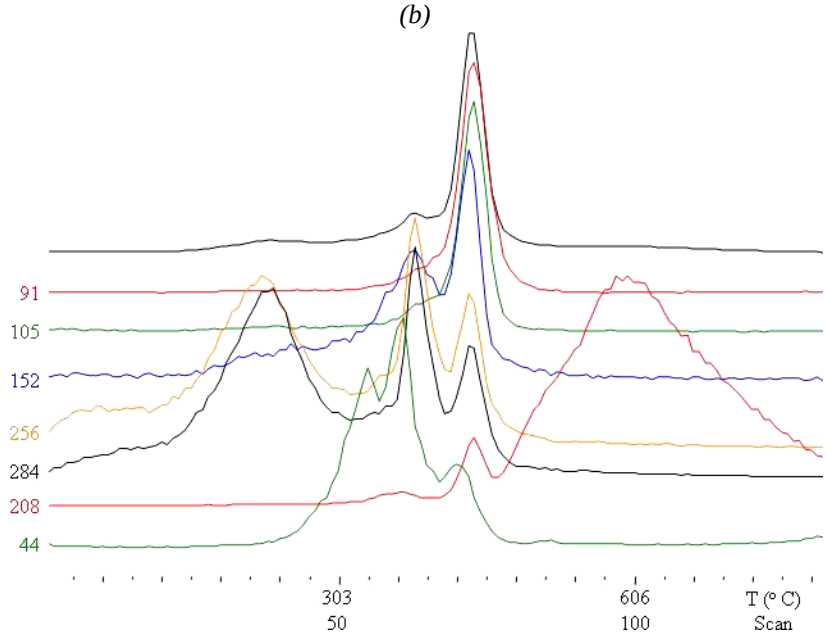

(c)

Fig. 5 – Mordant sample M10 (a) EI-DT summation mass spectrum (b) EI-DT mass spectrum of the pyrolysis region (temperature 406-467°C, scans 67-77) (c) TIC and mass thermograms of ion peaks at m/z 91 and 105 (alkylated benzenes), m/z 152 (C9 diacid), m/z 256 (C16:0 FA), m/z 284 (C18:0 FA), m/z 208 (Pb), and m/z 44 (CO_2)

A number of protein-derived mass peaks are also observed in all cases in the pyrolysis region of the TICs (Fig. 5b). In particular, the fragment ions at *m/z* 117 (indole), 131 (methylindole), and 145 (ethylindole) are produced by pyrolysis of tryptophan, and those at *m/z* 94 (phenol), 108 (methylphenol) and 186 [4-(4-hydroxyphenyl)-phenol] are pyrolytic products of tyrosine. These reveal the presence in the mordants of proteinaceous material [15].

Lastly, the mass peaks at *m/z* 206, 207, and 208 for the three isotopes of lead are present in the pyrolysis/organic as well as the high temperature/inorganic regions of the TICs. The former suggests that all mordants contain a lead-containing drier, whereas the latter together with the molecular ion peak of carbon dioxide (CO_2) at *m/z* 44 can be attributed to the thermal breakdown of basic lead carbonate [$2PbCO_3.Pb(OH)_2$] (Fig. 5) [11]. This is the commonly used pigment of lead white [16].

In the case of analysis under NH_3/CI conditions, the quasi-molecular ions at *m/z* 206, 220, 234, 248, 262, and 276 were detected in the summation mass spectra, corresponding to the C7, C8, C9, C10, C11, and C12 methylated diacids (Fig. 6). This ion pattern indicates that, in those cases, the oil used for the preparation of the mordants has been pre-polymerised, a process that yields a product of increased viscosity and higher degree of tackiness [17].

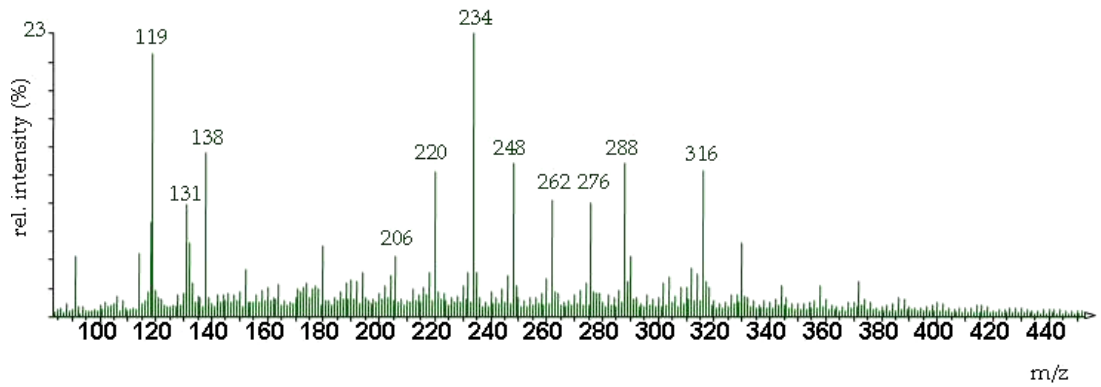

Fig. 6 – NH_3/CI-DT summation mass spectrum of the mordant sample S5

SEM-EDX

The elemental composition of some cross-sections was examined by single point EDX and EDX mapping (Fig. 7b-e). The mordant layers appear to contain carbon, amongst other elements, suggesting the presence of organic material. Lead was also detected, indicating the presence of a lead pigment, to act as dryer and/or filler. Other elements identified are primarily silicon and secondarily aluminium, iron, and oxygen (Fig. 7c-e). This composition refers to an alumino-silicate, which is mainly found in earth pigments and clays [18]. The latter appear in the microscopic images in the form of lumps of various shapes and sizes, and may have been added for their strong colour effect on the mordants (Figs. 2-4). The white layer that corresponds to the layer of modelling of the garments (Fig. 3a,b) consists of lead and, given the morphology of the particles as seen in the BSE image (Fig. 7a, layer b), it can be inferred that lead white was used for its preparation (Fig. 7c). Finally, the gold leaf was identified as being pure gold (Fig. 7b).

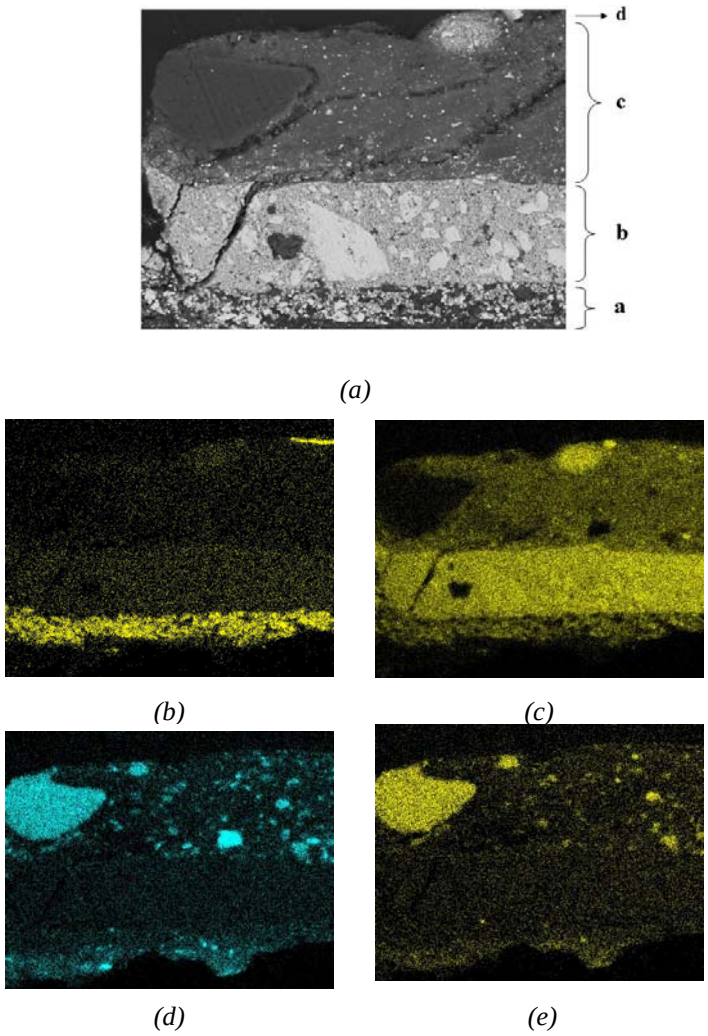

Fig. 7 – Cross-section S13 (a) BSE image; EDX mapping of (b) Au (c) Pb (d) Si (e) Al

CONCLUSION

The comparison of the findings from the main churches of the three monasteries in question demonstrates that both the materials used and the painting technique employed are similar. First, with regard to the cross-sections, the paint layers observed below the mordant in all three categories of gilded decoration follow largely the same build-up (Figs. 2-4). In addition, the mordants in all cases have similar chemical composition (Figs.5-7). It can therefore be concluded that, despite some expected differences owing to the variability of the samples, the gilded decoration of the wall paintings in the three monasteries was prepared according to the same methodology. Hence, it is quite likely that this was carried out by the same painter, possibly Tzortzis, or the same workshop.

ACKNOWLEDGEMENTS

The majority of analysis described in the present study was carried out at the laboratories of the FOM Institute for Atomic and Molecular Physics, Amsterdam, The Netherlands. The Greek State Scholarships Foundation provided Olga Katsibiri with a full scholarship. The 7th Superintendence of Byzantine Antiquities, the Transfiguration and the Roussanos Monasteries at Meteora and the St. Byssarionas Monastery at Doussiko are thanked for permission to take samples. We would also like to thank Marios Mitsatsikas for assistance with sampling.

REFERENCES

1. Winfield, D.C., Middle and Later Byzantine Wall Painting Methods - A Comparative Study, Dumbarton Oaks Papers, 22 (1968), 61-139.
2. Nikonanos, N., Meteora - A Complete Guide to the Monasteries and Their History, Ekdotike Athenon, Athens (1992), pp. 32-33.
3. Sofianos, D.Z., Tsigaridas, E.N., Holy Meteora - The Monastery of St. Nicholas Anapafsas: History and Art, Tsarouchas Bros, Kalambaka (2003), p. 104.
4. Acheimastou-Potamianou, M., Greek Art - Byzantine Wall Paintings, Ekdotike Athenon, Athens (1994), p. 261.
5. Choulia, S., Albani, J., Meteora: Architecture - Painting, Adam Editions, Athens (1999), pp. 91-110.
6. Nikonanos, N., op. cit., pp. 25-33.
7. Chatzidakis, M., Sofianos, D., The Great Meteoron - History and Art, Athens (1990), pp. 33-43.
8. Choulia, S., Albani, J., op. cit., pp. 46-53.
9. Nikonanos, N., op. cit., pp. 67-71.
10. Khandekar, N., Preparation of Cross-Sections from Easel Paintings, Reviews in Conservation, 4 (2003), 52-63.
11. Van den Berg, J.D.J., Analytical Chemical Studies on Traditional Linseed Oil Paints, PhD Thesis, FOM-Institute AMOLF, University of Amsterdam (2002), pp. 89-130; (http://www.amolf.nl/publications/theses/).
12. Mills, J.S., White, R., The Organic Chemistry of Museum Objects, Butterworth-Heinemann, Oxford (1999), pp. 171-172.
13. Van den Berg, J.D.J., op. cit., pp. 39-52.
14. Ibid., p. 99.
15. Van Arendonk, J.J.M.C., Niemann, G.J., and Boon, J.J., The Effect of Enzymatic Removal of Proteins from Plant Leaf Material as Studied by Pyrolysis-Mass Spectrometry: Detection of Additional Protein Marker Fragment Ions, Journal for Analytical and Applied Pyrolysis, 42 (1997), 33-51.
16. Gettens, R.J., Kühn, H., and Chase, W.T., Lead White, in Artists' Pigments: A Handbook of their History and Characteristics, Vol. 2, edited by A. Roy, National Gallery of Art, Washington DC (1993), pp. 67-81.
17. Mills, J.S., White, R., Organic Mass Spectrometry of Art Materials: Work in Progress, National Gallery Technical Bulletin, 6 (1982), 3-18.
18. Gettens, R.J., Stout, G.L., Paintings Material: A Short Encyclopaedia, Dover Publications, New York (1966), pp. 98, 134.

Back to Top